Journal of Catalysis 263 (2009) 114–122

Contents lists available at ScienceDirect

Journal of Catalysis

www.elsevier.com/locate/jcat

CO_2 fixation into methanol at Cu/ZrO_2 interface from first principles kinetic Monte Carlo

Qian-Lin Tang, Qi-Jun Hong, Zhi-Pan Liu *

Shanghai Key Laboratory of Molecular Catalysis and Innovative Materials, Department of Chemistry, Center for Computational Science and Engineering, Fudan University, Shanghai 200433, China

ARTICLE INFO

Article history:
Received 4 December 2008
Revised 27 January 2009
Accepted 27 January 2009
Available online 14 February 2009

Keywords:
Carbon dioxide fixation
Copper–zirconia catalyst
Synergetic effect
Density functional theory
Kinetic Monte Carlo

ABSTRACT

The efficient fixation/utilization of CO_2 has been pursued by chemists for decades. In this work, the catalytic kinetics of CO_2 fixation to methanol over a binary catalyst Cu/ZrO_2 is investigated by first principles kinetic Monte Carlo simulation. A Cu/ZrO_2 interface model is first established and the reaction network of CO_2 hydrogenation is explored. In the Cu/ZrO_2 system two reaction channels to methanol are identified (i) a reverse water–gas shift reaction via CO_2 decomposition to CO and (ii) the well-regarded mechanism via a formate intermediate. The theoretical selectivity is determined to be 85% for methanol and 15% for CO. The removal of the oxidative species is kinetically slow. As a result, 87% of the interface sites are covered by these oxidative species, which oxidize the interface Cu. We show that the binding strength of O atom at the interface is a critical parameter determining the activity and selectivity of the catalyst.

1. Introduction

The hydrogenation of CO_2 over Cu/oxides received much recent attention for both the industrial importance and the environmental concerns to CO_2 emission [1]. The reaction is also of fundamental interests as it illustrates well the significance of the so-called synergy effect in activating the thermodynamically very stable CO_2 molecule [2,3]. However, because of the great complexity of reactions occurring on composite materials, to achieve the atomic level understanding on the synergy effect has been a long-standing challenge in heterogeneous catalysis. To date, the key questions in the field, such as how and where CO_2 is activated over Cu/oxide systems [2], remain elusive. Aiming to establish a detailed kinetics model for the synergetic promotion of metal/oxide systems, here we carried out the first kinetic Monte Carlo (kMC) simulation over a model system, namely, CO_2 fixation into methanol on Cu/ZrO_2 based on extensive first principles calculations.

Methanol synthesis from CO_2/H_2 is a desired way to utilize CO_2, where Cu dispersed on oxides, including ZnO, ZrO_2, Al_2O_3, MgO, TiO_2 and SiO_2, are the typical catalysts [4]. While Cu/ZnO systems were most often used in practice, Cu/ZrO_2 systems received special attention because of their mechanical and thermal stability and high specific surface area [2]. Up to now, two classes of reaction routes leading to methanol (H_3COH) were hotly debated in literatures, namely, via surface formate (HCOO) and via adsorbed CO. The formate, as detected by *in situ* infrared spectroscopy, was suggested to derive from the direct hydrogenation of CO_2 [5,6]. On the other hand, the route involving CO_2 decomposition appears also likely, which utilizes the reverse water–gas shift (RWGS) reaction ($CO_2 + H_2 \rightarrow CO + H_2O$) to generate CO that is followed by the conventional syngas-to-methanol conversion ($CO + 2H_2 \rightarrow H_3COH$) [7–9]. The RWGS mechanism can explain straightforwardly the selectivity problem in CO_2 hydrogenation, where CO is the major unwanted byproduct [10], whilst the formate mechanism suggests that CO may be from methanol decomposition [11].

Despite the controversy on the detailed mechanism, the reaction was generally regarded to occur at the Cu/oxide interface [7,12]. This is because CO_2 can adsorb on bare oxides and H_2 dissociates much more efficiently on bare Cu than on oxides [13]. However, the views on the active Cu phase at the interface were much diverted. According to X-ray diffraction measurement of CO_2 hydrogenation over Cu/ZrO_2, Köeppel et al. found that active copper is present predominantly as Cu^0 not Cu^+ [14]. In contrast, Cu^+ was identified in $Cu/ZnO/SiO_2$ catalysts by static low-energy ion scatter experiment and was suggested to be the active component [15]. However, the other groups suggested that Cu metal and low valence of Cu ($Cu^{\delta+}$ and Cu^+) may all affect the catalytic activity of Cu/oxide systems [4,16,17]. Such unsettled puzzles are in fact common in heterogeneous catalysis. It is believed that to resolve the geometrical and electronic structures of the active site is the first step towards the rational design of catalyst with high catalytic activity/selectivity.

* Corresponding author. Fax: +86 21 6564 2400.
E-mail address: zpliu@fudan.edu.cn (Z.-P. Liu).

0021-9517/$ – see front matter
doi:10.1016/j.jcat.2009.01.017

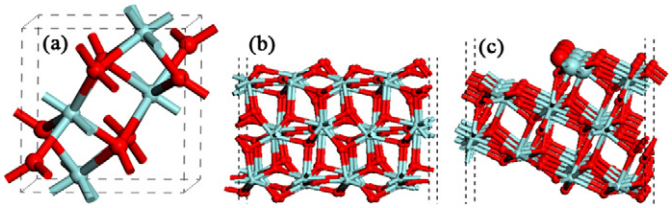

Fig. 1. (a) m-ZrO_2 crystal, (b) flat ($\bar{1}11$) surface, and (c) stepped ($\bar{2}12$) surface. O, red; Zr, cyan. (For interpretation of the references to color in this figure legend, the reader is referred to the web version of this article.)

Focusing on the atomic level detail of the interface catalysis, this work implemented the first statistical kinetics model to describe the hydrogenation of CO_2 at a Cu/ZrO_2 interface. The kinetic model relies on the first principles density functional theory (DFT) calculations, which were utilized to model the interface structure, explore the reaction network and provide the energetics of reaction steps. We show that dual reaction channels are present for CO_2 fixation into methanol at Cu/ZrO_2 interface. From the DFT results, kinetic Monte Carlo simulations were carried out to describe the steady state kinetics. The contribution of each reaction channel to methanol formation was thus assessed explicitly in terms of reaction rate. The kMC simulation demonstrates that methanol is produced through both the RWGS route and the formate route. Importantly, the catalytic activity and selectivity are shown to be intimately related to the interface binding ability towards oxidative species such as atomic O, as reflected by the apparently oxidized interface Cu.

2. Theoretical methodology

2.1. DFT calculation setups

All DFT periodic slab calculations were performed using SIESTA code [18]. The exchange-correlation functional utilized was at the level of Perdew–Burke–Ernzerf generalized gradient approximation [19]. For all elements, the basis set was expanded with the double-ξ plus polarization numerical atomic orbitals [20] and Troullier–Martins norm-conserving pseudopotential was used to treat the core electrons [21]. For Zr, the semi-core states (4s, 4p) have been included as valence states. A radii confinement of the orbitals was set as equivalent to an energy shift of 0.01 eV. The kinetic energy cutoff for the real-space mesh used to represent the density was specified to be 150 Ry. As the chosen supercells are rather large, only the Γ-point was employed for the first Brillouin-zone integration. Geometry optimization was performed by the Quasi–Newton–Broyden method until all the remaining forces acting on each relaxed atoms were below than 0.1 eV/Å. Transition states (TSs) of all the catalytic reactions were searched with our recently-developed constrained Broyden minimization method [22]. The convergence of our results was checked with respect to key DFT calculation parameters including the basis set, energy shift and kinetic energy cutoff, as summarized in Table S1 of the Supporting Information.

Monoclinic ZrO_2 (m-ZrO_2, Fig. 1a) was chosen as our model for the support since zirconia is one of the best oxide supports [4] and Cu/m-ZrO_2 was reported to have much higher activity and selectivity than Cu supported on tetragonal ZrO_2 (t-ZrO_2) for H_3COH synthesis from CO_2/H_2 [23]. Theoretically, the surface structure and stability of ZrO_2 (as measured by surface energy) were thoroughly investigated by Christensen et al. using the plane-wave DFT method [24]. They showed that the flat ($\bar{1}11$) facet (Fig. 1b) is the most stable surface of m-ZrO_2 and the stepped ($\bar{2}12$) facet (Fig. 1c) depicts the most common stepped sites. In our modeling, the two surfaces of monoclinic ZrO_2 were simulated by 3-layer slabs with a vacuum spacing of 16 Å. Large unit cells were employed: $p(2\times 2)$ [13.629 Å × 14.746 Å and 48 formula units of ZrO_2] for the ($\bar{1}11$) facet; $p(3\times 1)$ [20.443 Å × 11.693 Å and 54 formula units of ZrO_2] for the ($\bar{2}12$) facet. The topmost 16 ZrO_2 units and 24 ZrO_2 units were allowed to be relaxed for the two surfaces. Slab thickness was checked in order to achieve convergence—the difference of CO_2 adsorption energy calculated in the 3 and 4 layer slabs is at most 0.02 eV on each surface. To validate our DFT calculation setups, the chemical adsorption of CO_2 on bare m-ZrO_2 ($\bar{1}11$) (flat surface) and ($\bar{2}12$) (stepped surface) was first studied. The calculated CO_2 adsorption energy are 0.83 and 1.58 eV for the two surfaces, which are found to be in agreement with those determined by experiment (0.75–1.51 eV) [25]. The details on the modelling of Cu/ZrO_2 interface are addressed in Section 3.1.

2.2. Kinetic Monte Carlo setups

The kMC technique enables us to deal with complex heterogeneous catalytic phenomena on time scales of the order of seconds or ever longer, which cannot be achieved by typical molecular dynamics (MD) simulations [26,27]. For example, a previous kMC calculation of the partial oxidation of methanol on O/Cu(110) demonstrated that the kMC simulations are a powerful tool to give valuable insights into the complex details of the reaction kinetics on surfaces [28]. In this work we used the Bortz–Kalos–Lebowitz (BKL) kMC algorithm [29], which is briefly introduced as follows. The kMC algorithm enables a system to evolve in real time with dynamically varied system configurations. From a current configuration, kMC tells how to obtain the next system configuration and also how to calculate the time interval Δt between the two configurations. First, one should count all the possible events at the current configuration and calculate the rate of each event as $r(i)$ ($i = 1, 2, \ldots, n$, n is the total number of events). The total rate is obtained by $R = \sum_{i=1}^{n} r(i)$. Second, in the BKL algorithm, one can choose a random number $rand_1$ with a uniform distribution in the range $[0, 1)$, which is used to locate the kth event that satisfies the condition

$$\sum_{i=1}^{k} r(i) > R \times rand_1 > \sum_{i=1}^{k-1} r(i).$$

Finally, the event k will be selected to occur that leads to the next system configuration. The time interval between the two successive events (waiting time) is calculated as

$$\Delta t = -\frac{1}{R}\ln(rand_2),$$

where $rand_2$ is another random number in the range $[0, 1)$.

The rate r of an elementary event on a per site basis can be calculated based on transition state theory and statistical mechanics [30], as given by

$$r(T) = \frac{k_B T}{h} f^{TST}(T) \exp\left(-\frac{E_a}{K_B T}\right) = A \exp\left(-\frac{E_a}{K_B T}\right), \quad (1)$$

$$f^{TST}(T) = \frac{q^{TS}}{q^{IS}}, \quad (2)$$

where k_B is the Boltzmann constant, h is Planck's constant, f is the ratio of partition function q at the TS and that at the initial state (IS), A is the pre-exponential factor, and E_a is the reaction barrier, which can be calculated explicitly from DFT.

For surface reactions with Langmuir–Hinshelwood mechanism where the bond breaking-forming involves high-vibrational-frequency mode (such as C–H, O–H bonds), it can be shown that f is close to 1 because the entropy change (the vibrational partition function q_{vib} contribution) from the IS to the TS is nearly zero. In these cases, the pre-exponential factor A is about $k_B T/h$,

which is 10^{12}–10^{13} s^{-1} at typical temperatures. On the other hand, for the adsorption process (molecule from gas phase to surface), the pre-exponential factor is typically much smaller than 10^{13} s^{-1}, and f should be calculated explicitly. This is because the contributions from the translational and rotational partition functions of gas phase molecules significantly reduce the molecule sticking probability. The equations for calculating the rate of adsorption/desorption and surface reactions are detailed in supporting information.

3. Results and discussion

3.1. Reaction mechanism from DFT

Firstly, let us define the adsorption/binding energy of species X, $E_{ad}(X)$, as $E_{ad}(X) = E_{substrate} + E_X - E_{X/substrate}$, where E is the DFT total energy; a positive value of $E_{ad}(X)$ means the energy gain during adsorption. From our calculations, the binding energies of a Cu adatom at $ZrO_2(\bar{1}11)$ and $ZrO_2(\bar{2}12)$ are 0.99 and 1.08 eV, less than one third of the calculated cohesive energy of bulk Cu, 3.55 eV (experimental value 3.49 eV [31]). The growth of metallic Cu particles over the oxide surfaces is thus preferred thermodynamically, which is in line with the observation by transmission electron microscopy on Cu/oxides catalysts [32]. However, it should be borne in mind that the presence of metallic Cu particle does not exclude the possibility that Cu particles can be partly oxidized during the reaction so as that the interface Cu becomes ionic.

To represent the atomistic structure of the Cu/ZrO_2 interface, we added a two-layer close-packed Cu strip onto the $(\bar{2}12)$ stepped surface because the stepped oxide can provide a better geometry for both the adsorption of the Cu strip and reactant CO_2. It was reported that metal cationic monomers and metal particles anchor preferentially at oxide defected sites [33,34]. Furthermore, our DFT calculations for CO_2 adsorption on bare ZrO_2 also showed that CO_2 adsorbs more strongly at the stepped ZrO_2 than at the flat ZrO_2, which implies that the defected ZrO_2 is chemically more active in activating CO_2. A large unit cell was utilized to allow for a better lattice match between Cu and ZrO_2 (mismatch ≈0.4%, referred to the direction along the Cu strip, i.e., eight Cu–Cu lattice distances with respect to six Zr–Zr distances in bulk ZrO_2 lattice). The structure of the Cu/ZrO_2 system was firstly relaxed by first principles molecular dynamics with Nose thermostat at 200 K for ~1 ps; the energetically favorable structures from the MD trajectories were then selected and optimized by the Broyden method. The current interface model with a two-layer Cu strip should be enough to capture the chemistry of interface reactions as all the second-nearest neighboring atoms of the interface region have been included and fully relaxed. Additionally, we also checked the $H + CO_2 \rightarrow HCOO$ reaction by using an interface with a three-layer Cu strip and only 0.03 eV difference in barrier between two models is found.

Our optimized Cu/ZrO_2 interface is shown in Fig. 2a. This interface structure exposes only the most stable facets of the two components, i.e., the $(\bar{1}11)$ terrace of ZrO_2 and (111)-like Cu surface, which guarantees the structures to be energetically stable during the CO_2 hydrogenation reactions. We found that the Cu strip interacts mainly with the surface O_s of ZrO_2 with the newly formed Cu–O bonds being typically around 2.1 Å. The strength of each Cu–O bond is estimated to be 0.71 eV (i.e., Adsorption energy of the Cu strip divided by Number of Cu–O bonds). The interface between the oxide step-edge and the Cu strip can thus be viewed as an array of $(Zr)_2$–O–Cu linkages (see Fig. 2a), where the O is the original two-coordinated lattice O (O_{2c}) at the step-edge and the two Zr_s are five-coordinated (Zr_{5c}) and six-coordinated (Zr_{6c}) lattice Zr.

CO_2 adsorbs preferentially on the ZrO_2 sites of the Cu/ZrO_2 interface. The calculated adsorption energy (E_{ad}) of CO_2 is 0.69 eV.

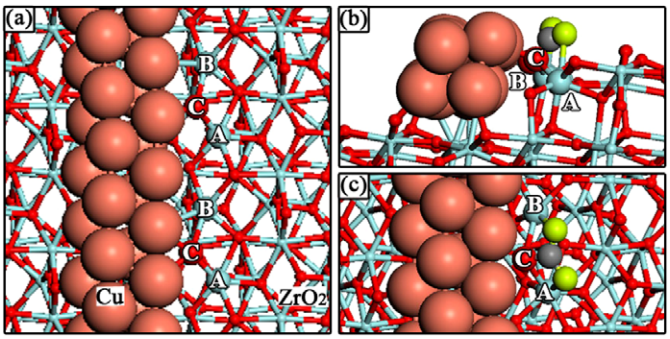

Fig. 2. (a) Optimized structure of Cu strip on stepped m-ZrO_2 $(\bar{2}12)$, and (b) side and (c) top views, respectively, of the structure of CO_2 adsorption. A, Zr_{6c}; B, Zr_{5c}; C, O_{2c}. Lattice O, red; Cu, orange; Zr, cyan; C, grey; O of CO_2, light green. (For interpretation of the references to color in this figure legend, the reader is referred to the web version of this article.)

The best configuration of CO_2 adsorption, as shown in Figs. 2b and 2c, features a tri-dented anchoring geometry: its two O and C atoms bond with the Zr_{6c}, Zr_{5c} and O_{2c}, respectively. The adsorbed CO_2 molecule thus lies nearly parallel to the $(\bar{1}11)$ plane with the O–C–O angle bent to 130.8°, as compared to the linearity of a free CO_2. Our Mulliken Charge analysis showed that upon adsorption, CO_2 is negatively charged by ~0.64 e. The extra electron is mainly transferred from the ZrO_2 support to the antibonding $2\pi_\mu$ orbital of CO_2 [35], apparently leading to the internal C–O bonds of CO_2 being much stretched (by ~0.1 Å). It should be noticed that the adsorption of CO_2 does not require the participation of Cu, which is distinct from O_2 adsorption in Au/ZrO_2 systems [33,34].

In contrast to CO_2 adsorption at the ZrO_2 side, we found that H atoms only adsorb strongly on the Cu side. The H atom adsorption energy at the Cu strip is 2.64 eV with respect to the gas phase H atom, which is much stronger than the H adatoms at the ZrO_2 side (1.76 eV) by forming OH with interface O_{2c}. This might not be surprising as ZrO_2 is hardly reducible [2]. In taking into account of the typical reaction conditions (at 500 K and 1.3 MPa the chemical potential of $1/2H_2$ in the gas phase is 2.49 eV lower with respect to the energy of a gas phase H atom), it is known thermodynamically that H atoms will prefer to adsorb on Cu and cannot diffuse to ZrO_2 via the interface O_{2c}. Kinetically, H_2 dissociation on Cu only requires a reaction barrier of 0.38 eV on the Cu strip, which is consistent with the general consensus that H_2 adsorbs dissociatively on Cu [36].

Next, we examined the reactions for CO_2 hydrogenation by starting from CO_2 at the ZrO_2 side and H at the Cu side of the interface. It should be born in mind that at present it is virtually impossible to provide an exhaustive first-principles account of the kinetics of a system of the complexity level as the CO_2 fixation. Nevertheless, in determining the reaction network, we took a trial-and-error iterative approach: (i) the likely reaction channels for a given intermediate are first examined; (ii) guided by the calculated reaction barriers, we only continue the low barrier reaction channels to reach the next new intermediate and reject the too high barrier ones (e.g., the barrier larger than 2 eV); and (iii) we repeat (i)–(ii) until methanol is produced. By this way, two routes leading to methanol, namely the formate route and the RWGS route as suggested by experiments [5–9], were both identified.

In total, 13 adsorbed species were found to involve in the catalytic paths, and their adsorption energies (E_{ad}) at the most stable site at the interface region are tabulated in Table 1 together with the nearest adsorbate-substrate bond distances. To provide a systematic overview of the PES of the species over the Cu/ZrO_2 model catalyst, the binding energies of these adsorbates are compared with their adsorption energies at the edge of the supported Cu strip and on Cu(111), namely, $E_{ad}^{Cu\text{-}edge}$ and $E_{ad}^{Cu(111)}$ (both sites are

Table 1
Adsorption energy E_{ad} (unit: eV) and the nearest adsorbate (A)–substrate (B) bond distances (unit: Å) for the species at the interface region (Figs. 3 and 4 for the adsorption structures) involved in DFT determined reaction paths.[a]

Species	A–B	$d_{A\text{-}B}$	E_{ad}	$E_{ad}^{Cu\text{-}edge}$	$E_{ad}^{Cu(111)}$	$E_{ad} - E_{ad}^{Cu(111)}$
H	H–Cu	1.73/1.74	2.64	2.64	2.43	0.21
O	O–Cu	1.96/1.99	6.63	4.92	4.62	2.01
	O–Zr	1.97				
OH	O–Cu	2.09	4.32	3.29	3.18	1.14
	O–Zr	2.17				
CO	C–Cu	1.95/2.00	1.07	1.07	0.91	0.16
CO_2	C–O	1.40	0.69	0.06	0.15	0.54
	O–Zr	2.28/2.34				
H_2O	O–Zr	2.40	0.72	0.40	0.18	0.54
HCO	C–Cu	2.01/2.02	2.51	1.61	1.56	0.95
	O–Zr	2.17				
HCOO	O–Zr	2.23/2.27	3.97	3.00	2.98	0.99
H_2CO	C–Cu	1.98	1.28	0.40	0.24	1.04
	O–Cu	2.19				
	O–Zr	2.14				
H_2COO	O–Cu	2.12	5.92	3.44	3.23	2.69
	O–Zr	2.03/2.12				
H_3CO	O–Cu	2.19/2.19	3.54	2.60	2.40	1.14
	O–Zr	2.13				
H_2COOH	O–Cu	2.24	3.41	2.08	1.7	1.71
	O–Zr	2.16/2.34				
CH_3OH	O–Zr	2.39	0.71	0.31	0.20	0.51

[a] For comparison their adsorption energies on the Cu strip $E_{ad}^{Cu\text{-}edge}$ and on Cu (111) $E_{ad}^{Cu(111)}$ are also listed. In calculations on Cu(111), a four-layer slab with a $p(2 \times 2)$ or $p(3 \times 2)$ surface unit cell was adopted with the topmost two layers relaxed.

Cu-only sites). Except for H_2COO and H_2COOH, the adsorption of the species on Cu(111) have been investigated within the DFT-GGA framework [37–39]. Our results on Cu(111) ($E_{ad}^{Cu(111)}$) are in good agreement with the previous reports.

For the H atoms and CO that adsorb preferentially at the Cu-only sites, E_{ad} is equivalent to $E_{ad}^{Cu\text{-}edge}$. For O, OH, HCO H_2CO, HCOO, H_2COO, H_3CO and H_2COOH intermediates, they all sit on ZrO_2 with their O ends, and most of them (except HCOO) simultaneously form bonding with the interface Cu atoms and the Zr atoms. For them, the adsorption energies at the Cu-only sites ($E_{ad}^{Cu\text{-}edge}$ or $E_{ad}^{Cu(111)}$) are generally much less than E_{ad} (by more than 0.95 eV), which indicates that the diffusion of these O-containing species over to Cu-only sites is unlikely. Interestingly, we found that $E_{ad}^{Cu\text{-}edge}$ is 0.1–0.4 eV greater than $E_{ad}^{Cu(111)}$, which implies that the lower-coordinated Cu at the edge of Cu strip is generally more active in binding with adsorbates compared to the close-packed Cu(111) surface.

In the following, the detailed mechanism of the two identified reaction routes is elaborated and their energy profiles are reported in Fig. 3.

3.1.1. Formate route

This route initiates by the direct hydrogenation of CO_2 to yield HCOO. At the TS (TS1, Fig. 3), the C–H bond distance is 1.73 Å and the calculated barrier height (E_a) is 0.46 eV. The low barrier is consistent with the strong exothermic nature of the reaction (1 eV). It implies that once CO_2 is captured via hydrogenation, the reverse reaction is unlikely to occur. Next, two more H can be sequentially added to form H_2COOH. In the process, the H atoms come from the Cu strip, while the CO_2 and its derivatives sit on the Zr sites. The internal C–O bond is weakened by the addition of H and it can break easily at the stage of H_2COOH, leading to the formation of H_2CO and OH. H_2CO can further be hydrogenated to H_3CO and finally H_3COH. It should be mentioned that H_2CO adsorbs strongly at the interface with a strong O–Zr bonding, but only weakly at Cu-only sites (Table 1). Considering that its hydrogenation barrier is only 0.44 eV, H_2CO at the interface would prefer hydrogenation rather than desorption or diffusion to Cu-only sites.

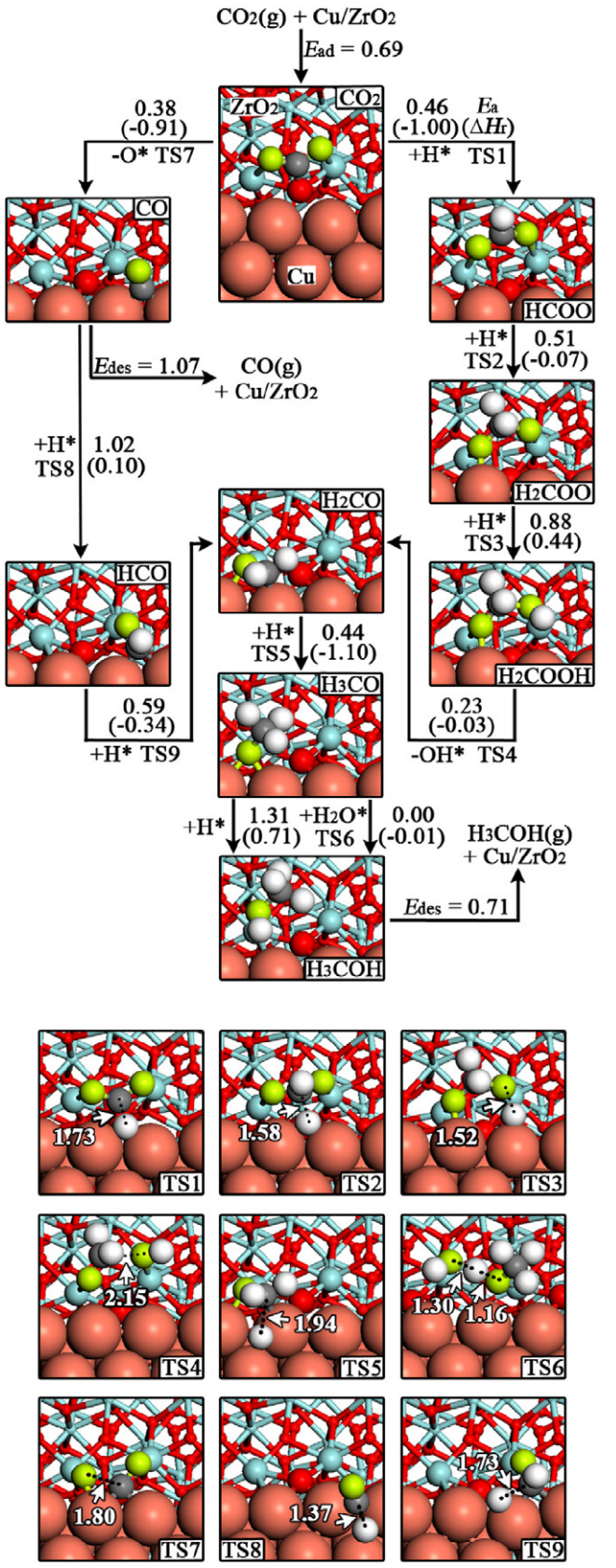

Fig. 3. Reaction network and the intermediates for methanol synthesis from CO_2/H_2 over the Cu/ZrO_2 interface. X* denotes an adsorbed species X. Key distances (Å) at TSs are labeled. Lattice O, red; Cu, orange; Zr, cyan; H, white; C, grey; O in reaction (non-lattice O), light green. The unit of energy is eV. (For interpretation of the references to color in this figure legend, the reader is referred to the web version of this article.)

From H_3CO to H_3COH, the direct hydrogenation ($H + H_3CO \rightarrow H_3COH$) at the interface is very difficult with a reaction barrier being 1.31 eV. In addition, we found that the H_3CO direct hydrogenation on the Cu strip also possesses a high reaction barrier of 1.01 eV. This implies that the diffusion of H_3CO onto the Cu side (requiring 1.14 eV, see Table 1) followed by the hydrogenation therein is also energetically hindered. However, we found that the hydrolysis channel ($H_2O + H_3CO \rightarrow OH + H_3COH$) at the interface is not only kinetically but also thermodynamically much more favorable. The hydrolysis path is essentially a non-barrier thermoneutral process. The facile hydrolysis reaction may not be surprising as it is essentially an intermolecular proton exchange process, where the breaking and forming O–H bonds at the TS (TS6) are determined to be as short as 1.30 and 1.16 Å, respectively. Our results confirm that the hydrolysis route is important to methanol formation, which has been proposed by experiment to explain why the addition of CO_2 will speed up the syngas-to-methanol conversion (CO/H_2 to methanol) [13].

It is worth mentioning that the cleavage of the C–O bond of H_3CO to yield CH_3 and O is very difficult with a barrier of 1.53 eV, even higher than the direct hydrogenation of H_3CO. This means that the production of byproduct methane (CH_4) is kinetically inhibited. This agrees with the experimental finding that CO_2 hydrogenation hardly has any selectivity to CH_4 over Cu/ZrO_2 [40,41].

In the stepwise hydrogenation process, the CH bond formation is generally preferred over the OH bond formation, which, we found, is controlled by thermodynamics. As shown in Fig. 3, the former reactions are either exothermic or thermoneutral, whilst the latter reactions are often endothermic. For example, the hydrogenation of HCOO can lead to either H_2COO or HCOOH. Although HCOOH (acetic acid) is a more common molecule, the OH bond formation at the interface is actually endothermic by 0.85 eV. By contrast, the formation of H_2COO is slightly exothermic by 0.07 eV. Consistently, the hydrogenation barriers to the CH bond formation are low (0.46, 0.51 and 0.44 eV for the hydrogenation of CO_2, HCOO and H_2CO, respectively), but the hydrogenation barriers to the OH bond formation are high (0.88 and 1.31 eV for the hydrogenation of H_2COO and H_3CO, respectively). This could be a general feature for catalysis at metal/oxide interface, where the O-end of intermediates affiliates strongly to the cationic site of oxides due to the electrostatic attraction and thus appears quite inert.

3.1.2. RWGS route

Alternative to CO_2 direct hydrogenation, CO_2 can undergo decomposition at the interface, i.e., $CO_2 \rightarrow CO + O$. The calculated reaction barrier of CO_2 splitting is 0.38 eV, slightly lower than the direct hydrogenation of CO_2 (0.46 eV). While no direct data on Cu/ZrO_2 system is available for comparison, we noticed that Elliott et al. did detect CO_2 decomposition on $Cu/ZnO/Al_2O_3$ catalysts within the temperature range of 173–513 K using mass spectrometer [42,43]. Our determined dissociation barrier, 0.38 eV, is lower than the experimental values determined over $Cu/ZnO/Al_2O_3$, 0.47–0.96 eV [42], which implies that ZrO_2 is an even more active oxide than ZnO/Al_2O_3. It is worth mentioning that the existence of CO_2 decomposition channel demonstrates the synergetic promotion of the Cu/ZrO_2 system: on single crystal Cu it is unlikely to thermally destroy CO_2 because the splitting of CO_2 into CO and lattice oxygen in bulk Cu_2O/CuO is strongly endothermic by 1.32/1.20 eV [42]. By contrast, the CO_2 decomposition on Cu/ZrO_2 was found to be highly exothermic because the interface O is rather stable with E_{ad} being 3.36 eV with respect to 1/2 O_2 in the gas phase. This magnitude is about 1.71 eV larger than the O atoms adsorbed on bare Cu sites.

After CO_2 dissociation, the produced CO shifts to the edge sites of Cu strip and the atomic O forms a new linkage between Zr_{5c} and Cu with Zr(or Cu)–O bonds being around 2.0 Å. Next, CO can either desorb to the gas phase from the Cu sites, or be hydrogenated progressively at the interface leading to methanol (via HCO, H_2CO and H_3CO). Energetically, the two processes are competitive: the CO desorption requires 1.07 eV, while the CO + H reaction has to overcome a barrier of 1.02 eV. It is worth mentioning that CO is hardly hydrogenated on Cu(111) with a high reaction barrier (1.21 eV) because HCO there is highly unstable ($CO + H \rightarrow HCO$ reaction on Cu(111) is endothermic by 0.89 eV) [39]. The produced HCO species can be facilely converted to H_2CO, with E_a of 0.59 eV and the reaction is exothermic by 0.34 eV. It can also be noticed that the RWGS route and the formate route share the common intermediates H_2CO and H_3CO.

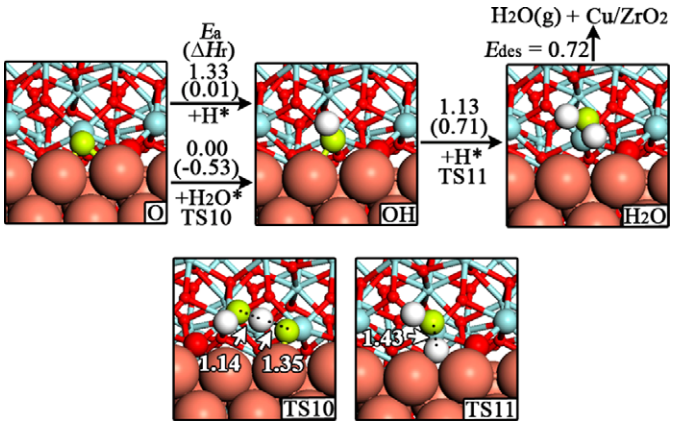

Fig. 4. Reaction path for the O removal ($O \rightarrow OH \rightarrow H_2O$) reactions at the Cu/ZrO_2 interface. X^* denotes an adsorbed species X. Key distances (Å) at TSs are labeled. Lattice O, red; Cu, orange; Zr, cyan; H, white; O in reaction, light green. The unit of energy is eV. (For interpretation of the references to color in this figure legend, the reader is referred to the web version of this article.)

A key feature of the RWGS route is the production of atomic O as additional linkages at the interface. Since the interface O is much more stable than the O atoms adsorbed on bare Cu sites, it might be interesting to ask whether the interface O will block the catalytic sites and eventually poison the catalyst. To answer this, we continued to scrutinize the possible pathways of the O removal, which are summarized in Fig. 4. Indeed, we found that the direct hydrogenation of the interface O is kinetically difficult with a high barrier (1.33 eV). By contrast, the hydrolysis route by $H_2O + O \rightarrow 2OH$ at the interface is again more likely with essentially no barrier by passing a proton exchange TS (TS10, Fig. 4), where the forming/breaking O–H bond distances are short, being 1.35 and 1.14 Å, respectively. Although the hydrolysis route can facilitate the O to OH conversion, the subsequent H_2O releasing by OH + H coupling still needs to overcome a 1.13 eV barrier, which implies that O removal is a kinetically slow process under reaction conditions.

It is of interest to further check whether the interface O atoms or OH groups can be removed by other reductive species. To this end, we have evaluated the reactions for $CO + O \rightarrow CO_2$ (the reverse reaction of CO_2 dissociation) and $CO + OH \rightarrow HOCO$, and both of them are highly endothermic (CO + O: 0.91 eV; CO + OH: 1.35 eV). Consistently, the CO + O reaction needs to overcome 1.29 eV barrier, which is higher than the barrier of CO + H reaction at the interface and also the CO adsorption energy. Experiment has been shown that the addition of CO into CO_2/H_2 methanol synthesis will poison the conversion [16], which is consistent with our finding that CO is unlikely to help the removal of interface O species. On the other hand, the diffusion of the interface O and OH to the Cu-only sites (Cu strip and Cu(111)) has to overcome at least 1.14 eV potential energy difference (Table 1) and the OH + H reaction on the Cu strip is also a highly activated process with a barrier 0.97 eV. Therefore, it can be concluded that the removal of

interface O atoms and OH through the other channels, including CO oxidation and diffusion to Cu sites, is energetically unfavorable.

In short, methanol synthesis from CO_2/H_2 mixture over Cu/ZrO_2 demonstrates well the synergetic effect between the Cu and ZrO_2. Initially, ZrO_2 acts as the adsorption site for CO_2, whilst H_2 dissociates on the Cu side. At the interface, the hydrogenation of CO_2 is competing with the direct CO_2 dissociation, which leads to two distinct paths to methanol. A number of elementary steps and intermediates are involved in this complex process, as shown in Fig. 3. It is therefore of significance to assemble all the pieces of information from DFT into a solid kinetic model to yield a more complete microscopic description on the origin of the activity and selectivity.

3.2. kMC simulations

With the whole reaction network being determined, we are in the position to assess which reaction route dominates the methanol formation and what is the theoretical selectivity. kMC simulation based on the elementary steps obtained from first principle calculations is an ideal approach to answer these questions. However, a full-scale kMC simulation to take into account all the sites on catalyst, including Cu and ZrO_2 sites, is a formidable task to compute, and obviously, a simplified model without much loss of the generality and the accuracy is necessary. By considering the information from DFT, we found that the kinetics of the interface catalysis may be reasonably described by a one-dimensional kMC lattice model since the catalytic process, in spite of the overall complexity, involves mainly the interface Zr sites (along a one-dimensional chain). In our one-dimensional lattice model, each lattice can be viewed as a Zr site at the interface; and every two neighboring lattice sites, namely A site (Zr_{6c}) and B site (Zr_{5c}) (see Fig. 2a), represent a potential location for CO_2 adsorption and the subsequent reactions.We have explicitly considered 21 elementary reaction steps, including the diffusion of H_2O and H_3COH along the interfacial oxide sites, as listed in Table 2, where the DFT calculated reaction barriers utilized have been tabulated. Although a full-scale kMC simulation that considers all the possible events, including diffusion and all reactions on Cu sites, is too demanding to perform as a benchmark, our one-dimensional model for the interface catalysis may still be largely validated for the following three considerations.

First of all, it is energetically unfavorable for the interface O-containing unsaturated species (such as O atoms, OH, HCOO and H_3CO) to diffuse either away from the interface to the Cu-only sites or along the interface sites. These species are very unstable at the Cu-only sites; and even if they happen to diffuse to the Cu-only sites, the following hydrogenation reactions remain to be kinetically difficult (e.g., $OH + H \rightarrow H_2O$ on Cu-only sites possess a barrier of 0.97 eV). In addition, each Zr site at the interface is well separated by lattice Os with the direct distance being about 3.5 Å. As these O-containing species bond strongly with one or two Zr atoms at the interface, it is also unlikely to allow for their diffusion along the interface by hopping from one Zr to another: from our calculations, the OH and H_3CO species can only diffuse unless they desorb first as radical-like species (their diffusion barrier are typically more than 2 eV).

Second, we found that H adatoms on Cu can reach thermodynamic equilibrium facilely in the context of slow interface hydrogenation/dehydrogenation reactions. The diffusion barrier of H on Cu(111) is very low (~0.15 eV on Cu(111)) [44], while the hydrogenation/dehydrogenation reactions occurring at the interface have barriers of at least 0.42 eV. According to the rate equation, the diffusion of H on Cu is at least 2–3 orders of magnitude faster than the hydrogenation or dehydrogenation processes at the interface at 500 K. Therefore, while one such interface event happens, the H on Cu must nearly reach equilibrium. Statistically, it is reasonable to treat the H atoms (and the vacant sites) on Cu implicitly in the rate equations as follows.

Table 2
Forward (E_f) and reverse (E_r) activation energy (unit: eV) of 21 elementary steps in kMC simulation of H_3COH synthesis from CO_2/H_2 over Cu/ZrO_2.[a]

Elementary step	E_f	E_r
$CO_2(g) + * \leftrightarrow CO_2^*$	0	0.69
$CO_2^* + * \leftrightarrow CO^* + O^*$	0.27[b]	1.29
$CO^* + H^* \leftrightarrow HCO^* + *$	0.98[b]	0.92
$HCO^* + H^* \leftrightarrow H_2CO^* + *$	0.59	0.93
$CO^* \rightarrow CO(g) + *$	1.07	–[c]
$CO_2^* + H^* \leftrightarrow HCOO^* + *$	0.43[b]	1.46
$HCOO^* + H^* \leftrightarrow H_2COO^* + *$	0.51	0.58
$H_2COO^* + H^* \leftrightarrow H_2COOH^* + *$	0.88	0.44
$H_2COOH^* + * \leftrightarrow H_2CO^* + OH^*$	0.23	0.26
$H_2CO^* + H^* \leftrightarrow H_3CO^* + *$	0.44	1.54
$H_2CO^* \leftrightarrow H_2CO(g) + *$	1.28	0
$H_3CO^* + H^* \leftrightarrow H_3COH^* + *$	1.31	0.60
$H_3COH^* \rightarrow H_3COH(g) + *$	0.71	–[c]
$O^* + H^* \leftrightarrow OH^* + *$	1.33	1.32
$OH^* + H^* \leftrightarrow H_2O^* + *$	1.13	0.42
$H_2O^* \rightarrow H_2O(g) + *$	0.72	–[c]
$H_2O^* + O^* \leftrightarrow OH^* + OH^*$	0.00	0.53
$H_2O^* + H_3CO^* \leftrightarrow OH^* + H_3COH^*$	0.00	0.01
$O^* + H_3COH^* \leftrightarrow OH^* + H_3CO^*$	0.00	0.70
$H_2O^* + * \leftrightarrow * + H_2O^*$[d]	0.45	0.45
$H_3COH^* + * \leftrightarrow * + H_3COH^*$[d]	0.46	0.46

[a] CO_2 adsorption has a low pre-exponential factor of 2.2×10^3 s^{-1} because of the large entropy of the gas phase CO_2 and the pre-exponential factor for all the other surface elementary reactions is 1.04×10^{13} s^{-1} from Eq. (1).

[b] The zero point energy correction is included for the reactions that are important to the methanol/CO selectivity.

[c] The readsorption of products (CO, H_3COH and H_2O) is not considered in order to obtain the theoretical selectivity without the interference of secondary reactions (namely, the product readsorption/decomposition).

[d] The diffusion of the two species occurs along the interfacial oxide sites.

For reactions involving a second site on the Cu side, we can calculate the rate $r'(T)$ by the following formula assuming the H-equilibrium at the Cu side:

$$r_i'(T) = \begin{cases} r_i(T), & \rho \leqslant \theta, \\ 0, & \rho > \theta, \end{cases}$$

where ρ is a random number with a uniform distribution in the range $[0, 1)$ and θ is the coverage of H atoms (θ_H) or vacant sites (θ_{vac}) on Cu. This means that, for example, the rate for a hydrogenation reaction is as that computed from Eq. (1) if the random number ρ is not higher than the H atom coverage; otherwise, the rate would be set to zero. In fact, at typical reaction conditions (H_2 at 500 K/1.3 MPa), it can be deduced that the H atom coverage at the interface region of the Cu side is rather high, more than 0.97, because the chemical potential of 1/2 H_2 in the gas phase is 0.15 eV less than the H atom adsorption energy at the interface region. During our kMC simulation, we have tested explicitly two cases where $\theta_H = 0.99$ and 0.90. We found that the catalytic selectivity and the occupancy of interface sites are little affected (within 3%).

Third, the adsorption of CO at the edge of the Cu strip restricts geometrically any other species to occupy its nearest Zr site. This is consistent with the fact that CO can easily tilt down with its O end attaching to the nearest Zr site during CO hydrogenation. This feature enables that CO, although adsorbs on the Cu strip, can be fitted into the one-dimensional lattice model by solely taking one lattice site. In addition, CO diffusion away from the Cu-edge (and subsequent desorption from Cu(111)) is considered to be not important for the following three facts: (i) CO adsorption at the edge of the Cu strip is stronger than it on Cu(111) by 0.16 eV (this means that the rate of a CO away from the interface is 40 times lower than it back to the interface at 500 K); (ii) CO is hardly hy-

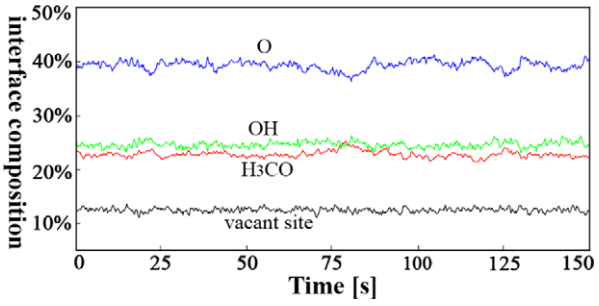

Fig. 5. Steady state interface composition averaged from 200 kinetic Monte Carlo trajectories.

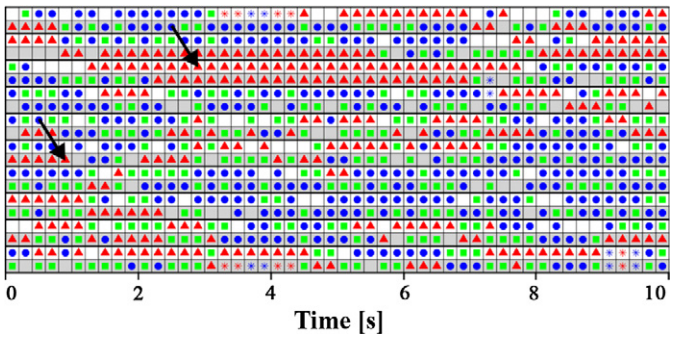

Fig. 6. Interface snapshots taken every 0.2 s from a single 10-s kinetic Monte Carlo trajectory. The major species are O (sphere), OH (square) and H_3CO (triangle). The lattice (the column) contains 10 pairs of A site (Zr_{6c}, white) and B site (Zr_{5c}, grey). Pairs are separated by darker lines.

drogenated on Cu(111) (see Section 3.1) [39] and (iii) CO diffusion away from the interface is kinetically hindered at typical reaction conditions as the H coverage on Cu (i.e., nearby CO) is rather high, as mentioned above. Overall, for one produced CO at an interface Cu site, the probability of neighboring vacant sites on Cu is less than 3% due to high H coverage. Moreover, even at such 3% situations, the probability of the CO will eventually be at the vacant site is about 1/40. Therefore, it is reasonable to neglect the CO diffusion away from interface Cu site. The same argument can also be applied to understand that H_2O diffusion is unlikely from the interface to the Cu site.

Perhaps the most perplexing issue in kMC modeling is the treatment of lateral interaction between intermediates. Fortunately, our case is in fact much simpler. This is to a large extent due to the fact that each Zr site is well separated by lattice Os with the direct distance being about 3.5 Å. This implies that the effect of the lateral interaction on the reaction barriers is small. Therefore, we only explicitly considered the lateral interaction for the key reaction steps that are important to the selectivity. We have calculated the two key reactions, say, $CO_2 + H \rightarrow HCOO$ and $CO_2 \rightarrow CO + O$, in the presence of one neighboring O atom or H_3CO species. The barriers for the two reactions are 0.31 and 0.32 eV in the presence of O, and 0.36 and 0.38 eV in the presence of H_3CO. The presence of these oxidative species changes the reaction barrier by at most 0.15 eV, which is indeed small by absolute value (comparable to the typical DFT error). However, we noticed that the barrier difference between the CO_2 hydrogenation and CO_2 splitting becomes smaller, which can affect the selectivity. (In our kMC simulations, zero point energy correction has been included on the barriers of the two reactions and the CO_2 splitting always has a lower barrier than the CO_2 hydrogenation, see Table 2.)

In our kMC simulation, we set the temperature at 500 K and the CO_2 partial pressure at 0.4 MPa, which are the typical conditions used in experiment for Cu/ZrO_2 catalysts [14]. Our lattice model for kMC is a one-dimensional chain with periodic boundary conditions imposed, which is composed of 10 pairs of 5-coordinated Zr and 6-coordinated Zr sites at the interface. Such a model was chosen to balance the accuracy and the efficiency. A larger lattice model containing 50-pair sites was also tested, which showed no significant difference in results. Our statistical results were obtained by averaging the output of 200 kMC runs (trajectories), each with 200 s ($\sim 10^9$ steps); the results are statistically converged as the standard uncertainty (i.e., estimated standard deviation) of the interface composition (see below) is below 3%. The steady state is achieved after about 50 s.

The statistical results from our kMC simulations are summarized as follows. As shown in Fig. 5, we found that at the steady state 87% of the interface sites are covered by oxidative species, including 39% atomic O, 25% OH and 23% H_3CO species, and 12% are vacant sites. The coverage of a species is with respect to the total interface sites, defined statistically by the $[\Sigma(n \times \Delta t)]/(t_{\text{total}} \times N_{\text{site}})$, where Δt is the time interval of each simulation step; n is the number of the species within a time interval Δt; t_{total} is the total time in simulation ($t_{\text{total}} = \sum \Delta t$) and N_{site} is the number of total sites (i.e., 20 in our simulation). The other surface intermediates with the concentration higher than 0.1% are only HCOO and H_2COO from kMC, which is simply due to the fact that HCOO and H_2COO are relatively stable species in the reaction map: neither the dissociation of HCOO to CO_2 and H nor the further hydrogenation of H_2COO to H_2COOH is thermodynamically favorable. Importantly, the calculated interface composition indicates that the interface Cu atoms are partly oxidized and the formal oxidation state of Cu is about +0.9 by average in our model. This means that the appearance of cationic Cu is just a natural consequence of the catalytic process. The *in situ* formation of cationic Cu seen from kMC simulation may help rationalize the experimental observations, where the ionic copper was identified during methanol synthesis from CO_2/H_2 [45,46].

The microscopic reaction pattern can be viewed from Fig. 6, where the interface snapshots are taken every 0.2 s from a single 10-s kMC trajectory. Although 12% of the surface sites is empty, it is in fact not easy to create a pair of adjacent vacant sites (Zr_{5c} and Zr_{6c}) that is needed for CO_2 adsorption: statistically, the population of such a pair of vacant sites is $\sim 10^{-5}$ of the total interface sites from kMC and therefore cannot be identified in the snapshots with a 0.2 s interval in Fig. 6. Obviously, it is undesirable to have too large bonding ability of Zr sites towards the O-containing species, which will introduce the competition for the interface sites between these species and CO_2. Considering that the interface sites are already in minority by themselves in a catalyst, the theory can thus predict the low conversion rate of CO_2 fixation *due to the lack of surface active sites*, although the barriers for CO_2 direct hydrogenation/decomposition are both low. This does agree with the general fact in experiment that the conversion ratio of CO_2 is typically below 10% but the measured barrier for methanol formation is not high [14].

Fig. 6 also shows some important fingerprints of the complex reaction network. Perhaps the most important one is that the hydrolysis route dominates clearly the formation of methanol. This can be seen by comparing the fate of two H_3CO as labeled by the arrows in the figure. The upper arrow points to a H_3CO neighboring with other two H_3CO, which keeps unchanged for a long period ($\sim$6 s). This is because the direct hydrogenation of H_3CO is kinetically slow ($E_a = 1.31$ eV) and it is not possible to pass proton from the neighboring H_3CO groups. The lower arrow points to a H_3CO that neighbors with adsorbed O and OH groups, which turns into methanol after a short period (1 s). According to our statistics, more than 99.99% of the methanol produced originates from the hydrolysis path via $H_2O + H_3CO \rightarrow OH + H_3COH$ and $OH + H_3CO \rightarrow O + H_3COH$.

Furthermore, the kMC simulation tells that methanol is mainly produced via the RWGS route (74%) with a minor contribution from the formate route (26%). The selectivity is obtained by counting the number of the produced methanol molecules from the two routes. Although HCOO and H_2COO are the major surface species apart from the oxidative species (O, OH and H_3CO), they are in fact not the key intermediates leading to methanol, which has been suggested by Weigel et al. according to the FTIR experiment [9]. Our determined selectivity to methanol is about 85%, which is accordance with the experimental values reported for typical Cu/ZrO_2 catalysts [6]. It however should be emphasized that the selectivity obtained here is based on DFT data, where a typical 0.2 eV error bar in the computed energy barrier is often present. Therefore, from our DFT results it might be more appropriate to state that the two major routes are equally important for CO_2 hydrogenation to methanol.

It should be emphasized that the presence of the RWGS route in the Cu/ZrO_2 catalyst leads inevitably to the unwanted CO. This is because the adsorption energy of CO on Cu is comparable to the barrier of CO hydrogenation. To further increase the selectivity to methanol, it would be ideal to increase the rate of $CO_2 + H$ reaction but slow the CO_2 splitting. By comparing the two reactions, we suggest that the bonding ability of atomic O with cationic Zr at the interface could be the key. According to the Brønsted–Evans–Polanyi relation [47,48], if the atomic O at the interface becomes less stable, it is conceivable that CO_2 dissociation will become slower. In contrast, the CO_2 direct hydrogenation would be less affected as only the bond between the C and the lattice O_{2c} breaks in the reaction and the O–Zr bonds remain untouched. As the interface O bonding strength is determined largely by the oxide support, it is thus possible to optimize the selectivity by varying oxide support, for example, replacing ZrO_2 by ZnO as done in practice [49]. Interestingly, the microscopic picture of the CO_2 fixation process revealed here indicates that the presence of interface oxidative species (or cationic Cu), being a reflection of the strong bonding of O at the interface, is an indication for both low activity and undesirable selectivity of the catalyst.

4. Conclusions

This work represents the first theoretical attempt to address the kinetics of a catalytic process occurring at metal/oxide interfaces, namely, CO_2 hydrogenation at Cu/ZrO_2 interface. Despite the complexity of the reaction network, which involves two reaction channels and many intermediates, we demonstrate that a simple one-dimensional kinetic model may be enough to capture the physical origin of the synergetic promotion in the composite system. Our results are summarized as follows.

Methanol is produced from both the RWGS route, which features the splitting of CO_2 to produce CO and atomic O at the interface, and the formate route. Because of the presence of CO_2 splitting route, the CO releasing as byproduct is inevitable as the CO hydrogenation barrier is quite comparable to the CO adsorption energy. Although HCOO and H_2COO can indeed be identified, they are not the key intermediate leading to methanol. The hydrolysis route plays important roles in methanol formation and O removal. The interface sites are largely occupied by oxidative species, such as O atoms, OH and H_3CO groups and, therefore, the interface Cu atoms are cationic. The low conversion rate of CO_2 fixation can be attributed to the lack of active sites for CO_2 adsorption/reaction, where a $(Zr)_2$–O–Cu interface linkage is necessary. To optimize the interface property by controlling the O-affinity of the oxide cationic site (e.g., acidity) could be the key to enhance CO_2 conversion rate and also to increase the selectivity. The picture presented here would benefit the rational catalyst design by tuning the interface properties, and maybe more importantly, provides the first hope for theory to solve the kinetics of complex catalytic process over multi-component materials.

Acknowledgments

This work is supported by NSF of China (20573023, 20773026, 20721063, J0730419) and Science & Technology Commission of Shanghai Municipality (08DZ2270500). Shanghai Supercomputing Center is thanked for computing time.

Supporting information available

The online version of this article contains additional supporting information: The rate equations for reaction used in kMC simulation; The convergence tests for some key species and key reactions with respect to DFT calculation parameters; Cartesian coordinates of the optimized Cu/ZrO_2 system, and Cartesian coordinates of three key reactions (CO_2 direct hydrogenation, CO_2 decomposition and CO hydrogenation).

Please visit DOI: 10.1016/j.jcat.2009.01.017.

References

[1] K.M.K. Yu, C.M.Y. Yeung, S.C. Tsang, J. Am. Chem. Soc. 129 (2007) 6360.
[2] X.-M. Liu, G.Q. Lu, Z.-F. Yan, J. Beltramini, Ind. Eng. Chem. Res. 42 (2003) 6518.
[3] J. Słoczyński, R. Grabowski, A. Kozłowska, P. Olszewski, J. Stoch, J. Skrzypek, M. Lachowska, Appl. Catal. A 278 (2004) 11.
[4] J.Y. Liu, J.L. Shi, D.H. He, Q.J. Zhang, X.H. Wu, Y. Liang, Q.M. Zhu, Appl. Catal. A 218 (2001) 113.
[5] K.-D. Jung, A.T. Bell, J. Catal. 193 (2000) 207.
[6] T.C. Schilke, I.A. Fisher, A.T. Bell, J. Catal. 184 (1999) 144.
[7] C. Schild, A. Wokaun, A. Baiker, J. Mol. Catal. 63 (1990) 243.
[8] J.R. Jennings, R.M. Lambert, R.M. Nix, G. Owend, D.G. Parker, Appl. Catal. 50 (1989) 157.
[9] J. Weigel, R.A. Koeppel, A. Baiker, A. Wokaun, Langmuir 12 (1996) 5319.
[10] J. Słoczyński, R. Grabowski, A. Kozłowska, P. Olszewski, M. Lachowska, J. Skrzypek, J. Stoch, Appl. Catal. A 249 (2003) 129.
[11] Y. Nitta, O. Suwata, Y. Ikeda, Y. Okamoto, T. Imanaka, Catal. Lett. 26 (1994) 345.
[12] Y. Borodko, G.A. Somorjai, Appl. Catal. A 186 (1999) 355.
[13] I.A. Fisher, A.T. Bell, J. Catal. 172 (1997) 222.
[14] R.A. Köeppel, A. Baiker, A. Wokaun, Appl. Catal. A 84 (1992) 77.
[15] W.P.A. Jansen, J. Beckers, J.C. van der Heuvel, A.W.D. van der Gon, A. Bliek, H.H. Brongersma, J. Catal. 210 (2002) 229.
[16] M. Saito, T. Fujitani, M. Takeuchi, T. Watanabe, Appl. Catal. A 138 (1996) 311.
[17] X.-M. Liu, G.Q. Lu, Z.-F. Yan, Appl. Catal. A 279 (2005) 241.
[18] J.M. Soler, E. Artacho, J.D. Gale, A. García, J. Junquera, P. Ordejón, D. Sánchez-Portal, J. Phys. Condens. Matter 14 (2002) 2745.
[19] J.P. Perdew, K. Burke, M. Ernzerhof, Phys. Rev. Lett. 77 (1996) 3865.
[20] E. Artacho, D. Sánchez-Portal, P. Ordejón, A. García, J.M. Soler, Phys. Status Solidi B 215 (1999) 809.
[21] N. Troullier, J.L. Martins, Phys. Rev. B 43 (1991) 1993.
[22] H.-F. Wang, Z.-P. Liu, J. Am. Chem. Soc. 130 (2008) 10996.
[23] K.T. Jung, A.T. Bell, Catal. Lett. 80 (2002) 63.
[24] A. Christensen, E.A. Carter, Phys. Rev. B 58 (1998) 8050.
[25] B. Bachiller-Baeza, I. Rodriguez-Ramos, A. Guerrero-Ruiz, Langmuir 14 (1998) 3556.
[26] K. Reuter, D. Frenkel, M. Scheffler, Phys. Rev. Lett. 93 (2004) 116105.
[27] K. Reuter, M. Scheffler, Phys. Rev. B 73 (2006) 045433.
[28] C. Sendner, S. Sakong, A. Groß, Surf. Sci. 600 (2006) 3258.
[29] A.B. Bortz, M.H. Kalos, J.L. Lebowitz, J. Comput. Phys. 17 (1975) 10.
[30] W.F.K. Wynne-Jones, H. Eyring, J. Chem. Phys. 3 (1935) 492.
[31] D.R. Alfonso, J.E. Jaffe, A.C. Hess, M. Gutowski, Phys. Rev. B 68 (2003) 155411.
[32] K. Taek, A.T. Bell, Catal. Lett. 80 (2002) 63.
[33] Z.-P. Liu, C.-M. Wang, K.-N. Fan, Angew. Chem. Int. Ed. 45 (2006) 6865.
[34] C.-M. Wang, K.-N. Fan, Z.-P. Liu, J. Am. Chem. Soc. 129 (2007) 2642.
[35] J.W. Rabalais, J.M. McDonald, V. Scherr, S.P. McGlynn, Chem. Rev. 71 (1971) 73.
[36] J. Wambach, A. Baiker, A. Wokaun, Phys. Chem. Chem. Phys. 1 (1999) 5071.
[37] A.A. Gokhale, J.A. Dumesic, M. Mavrikakis, J. Am. Chem. Soc. 130 (2008) 1402.
[38] J. Greeley, M. Mavrikakis, J. Catal. 208 (2002) 291.
[39] K.H. Lim, Z.-X. Chen, K.M. Neyman, N. Rösch, J. Phys. Chem. B 110 (2006) 14890.
[40] Y. Zhang, J. Fei, Y. Yu, X. Zheng, Energy Convers. Manage. 47 (2006) 3360.
[41] C. Yang, Z.Y. Ma, N. Zhao, W. Wei, T.D. Hu, Y.H. Sun, Catal. Today 115 (2006) 222.

[42] A.J. Elliott, M.J. Watson, J. Tabatabaei, F.W. Zemichael, K.C. Waugh, Catal. Lett. 79 (2002) 1.
[43] A.J. Elliott, R.A. Hadden, J. Tabatabaei, K.C. Waugh, F.W. Zemichael, J. Catal. 157 (1995) 153.
[44] J. Greeley, M. Mavrikakis, J. Phys. Chem. B 109 (2005) 3460.
[45] G.C. Chinchen, K.C. Waugh, D.A. Whan, Appl. Catal. 25 (1986) 101.
[46] S.-H. Liu, H.P. Wang, H.-C. Wang, Y.W. Yang, J. Electron Spectrosc. Relat. Phenom. 144 (2005) 373.
[47] N. Brønsted, Chem. Rev. 5 (1928) 231.
[48] M.G. Evans, N.P. Polanyi, Trans. Faraday Soc. 32 (1936) 1333.
[49] M. Saito, M. Takeuchi, T. Fujitani, J. Toyir, S. Luo, J. Wu, H. Mabuse, K. Ushikoshi, K. Mori, T. Watanabe, Appl. Organomet. Chem. 14 (2000) 763.